

Spatiotopic selectivity of BOLD responses to visual motion in human area MT

Giovanni d'Avossa^{1,2}, Michela Tosetti³, Sofia Crespi^{1,4}, Laura Biagi³, David C Burr^{5,6} & Maria Concetta Morrone¹

Many neurons in the monkey visual extrastriate cortex have receptive fields that are affected by gaze direction. In humans, psychophysical studies suggest that motion signals may be encoded in a spatiotopic fashion. Here we use functional magnetic resonance imaging to study spatial selectivity in the human middle temporal cortex (area MT or V5), an area that is clearly implicated in motion perception. The results show that the response of MT is modulated by gaze direction, generating a spatial selectivity based on screen rather than retinal coordinates. This area could be the neurophysiological substrate of the spatiotopic representation of motion signals.

Single-unit studies in the macaque have shown that in many cortical areas neuronal responses to visual stimuli are affected by gaze direction. Gaze direction can modulate neural response amplitude in a multiplicative fashion, referred to as a 'gain field'¹. Population coding of cells with gain fields could be important in localizing objects in external, or at least craniotopic, coordinates². In specific parietal areas, subpopulations of neurons have been described with spatiotopic (or at least craniotopic) receptive fields^{3–5} that change their retinotopic mapping with gaze. Areas where this property has been observed most clearly tend to serve polysensory functions^{6,7}, where the remapping is presumably necessary to integrate sensory input from different mobile sensor platforms^{8–10}. In some purely visual areas, however, receptive fields undergo transient remapping at or before the time of saccadic eye-movements^{11,12}. Remapping in eye-centered coordinates has also been observed across saccades in the human parietal cortex using imaging techniques¹³.

Psychophysical studies have demonstrated spatiotopic processing in the human visual system for several visual tasks¹⁴, some of them quite basic, that are mediated by low-level neural mechanisms. In particular, weak motion signals, delivered at different retinal locations but identical allocentric locations, can be integrated linearly over time to improve motion discrimination thresholds¹⁵. As evidence in nonhuman primates suggests that this type of motion discrimination task is mediated by area MT^{16,17}, the spatiotopic integration of motion signals implies that MT may encode motion in a spatiotopic fashion. In humans, the major neural station for visual motion processing is also referred to as MT (or V5)^{18–20} and is divided into two functional regions^{21–23}: one thought to be retinotopic (a possible homolog of macaque MT) and the other thought not to be retinotopic, with both

ipsilateral and contralateral responses (a possible homolog of macaque medial superior temporal cortex, MST). However, as previous studies have always mapped the visual response in human MT with gaze being held constant at the screen center, it remains unclear whether the response depends only on the stimulated portion of the retina or also on the position of stimuli in external space, which is given by both retinal position and gaze direction. In this case, the response should possibly be considered spatiotopic rather than retinotopic.

Imaging studies have shown that eye-position signals are present in human MT²⁴, although their effects on the neural response to visual stimuli have not yet been examined. Other studies show that in the anterior, nonretinotopic portion of human MT (the putative homolog of macaque MST), visual responses to complex flow patterns that simulate self-motion seem to be modulated by both retinal and eye-velocity signals in a manner consistent with encoding of rotational head motion²⁵, reinforcing previous suggestions from single-cell data²⁶. It therefore seems plausible that human MT may be implicated in the transformation of retinotopic to spatiotopic reference frames.

Here we examine directly whether the supposedly retinotopic portion of human MT has spatiotopic properties, making it the potential neural substrate for the spatiotopic integration of visual motion. The results show that the retinotopic selectivity does indeed change with eye position in a way consistent with spatiotopic representation of motion stimuli.

RESULTS

We first isolated the MT complex in each subject by comparing the response to large-field flow motion with the response to random motion during passive viewing. The retinotopic portion of this area

¹Facoltà di Psicologia, Università Vita-Salute 'San Raffaele', Via Olgettina 58, 20132 Milan, Italy. ²Washington University School of Medicine, 660 South Euclid Avenue, St. Louis, Missouri 63110, USA. ³Fondazione 'Stella Maris', Viale del Tirreno 331, 56018 Calambrone, Pisa, Italy. ⁴Department of Psychology, Università Degli Studi di Milano Bicocca, Viale dell'Innovazione, 10 20126 Milan, Italy. ⁵Department of Psychology, Università Degli Studi di Firenze, Via S. Niccolò 89 Florence, Italy. ⁶Department of Psychology, University of Western Australia, Stirling Hw., Nedlands Perth, Western Australia, Australia. Correspondence should be addressed to M.C.M. (concetta.morrone@hsr.it).

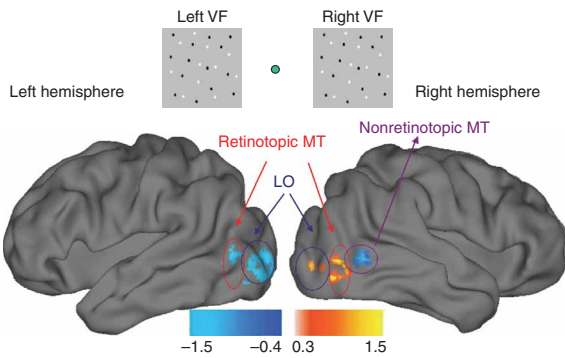


Figure 1 The maps highlight regions in the lateral occipitotemporal cortex that responded to optic flow for subject GA. In these regions, cold colors represent a left visual field preference and warm colors a right visual field preference. The values were obtained from z-transformed *t*-statistics of the magnitude difference of activations evoked by the two stimuli shown in the top panel. This map was smoothed with a uniform spherical kernel of 6 mm radius to improve the surface representation. The posterior region is part of the LO and the anterior region is part of the inferior temporal sulcus (MT). The right hemisphere MT had two separable portions: the posterior portion, showing a preference for the contralateral visual field, and the anterior, showing a weak preference for the ipsilateral visual field, presumably corresponding to MST. The upper cartoon shows the visual fields and the appearance of the position and size of the visual stimuli with respect to the fixation dot. **Table 1** shows the Talairach coordinates of the retinotopic portion of MT.

was then defined as those voxels that showed a strong contralateral preferential response to patches of randomly moving dots, alternating between the left and the right of fixation. We assessed the blood oxygenation level-dependent (BOLD) response to the flow stimuli displayed in the left versus the right visual field, projected on the inflated brain of one subject (**Fig. 1**). Two regions were activated along the posterior portion of the inferior temporal sulcus: a dorsal, anterior region that showed no preference for contralateral visual stimuli and a posterior, ventral region that did prefer contralateral over ipsilateral stimuli (see also ref. 21). The other separate, more posterior, region did not respond to flow against speed-matched random motion and probably belongs to the lateral occipital region (LO) rather than the MT complex²⁷. This region was not included in the analysis. The Talairach coordinates of the ‘retinotopic’ portions of MT for the seven subjects are reported in **Table 1**.

Widely spaced event-related design

We measured spatiotopic selectivity with two complementary techniques: a widely spaced event-related design and a blocked design. For the event-related design, visual stimuli lasted 6 s and contained brief motion sequences imbedded within dynamic random noise, at coherence levels near the discrimination threshold. Low coherence levels were used to ensure that the subjects’ attention was directed to the stimulus for its entire duration, as they were required to determine the direction of motion. We recorded time courses of responses for area V1 and the retinotopic portion of MT from a representative hemisphere of subject MCM, evoked by stimuli presented at matched retinal eccentricity under three conditions of fixation (**Fig. 2**). The upper panels show the response to ipsi- and contralateral stimuli presented left or right of a central fixation dot (the typical situation used by most studies^{22,23}). The patterns of responses in both V1 and MT were similar. In both areas there was a strong contralateral response, rising to a maximum 6–9 s after stimulus onset, whereas the ipsilateral response remained negligible, rarely rising above the baseline. The lower curves show the response for centrally displayed stimuli, where the retinal eccentricity of the stimulus was determined by changing the point of fixation (on which subjects maintained fixation for the entire session, with eye-position monitored to ensure compliance). With eccentric fixation, the pattern of BOLD responses in area V1 was similar to that observed with central fixation. However, the supposedly retinotopic portion of MT responded quite differently, with responses to ipsi- and contralateral retinal stimulation now virtually identical.

Figure 3 shows a summary of the results for each responsive hemisphere of the three subjects for areas V1 and MT. Each point is the average BOLD signal during the first 12 s following stimulus onset. Blue points indicate central gaze with eccentric stimuli and red points

indicate central stimuli with eccentric gaze. For V1, the response to the ipsilateral visual stimulus was always near zero, indicating that the response depended solely on the retinal eccentricity of the stimulus, rather than its position in space. The responses in MT, however, were quite different: for central fixation the response to ipsilateral stimuli was much less than the response to contralateral stimuli, but when the stimulus position was held constant and gaze varied the magnitudes of the ipsi- and contralateral responses were very similar. The red and blue lines in **Figure 3**, linear regressions of the data, quantify the effects of gaze, giving the average ratio of ipsilateral to contralateral responses. For MT this ratio was 0.91 ± 0.08 when the stimuli were displayed centrally, but only 0.26 ± 0.11 for peripherally displayed stimuli, with no overlap of the 95% confidence intervals. For V1, the ratio was near zero in both cases, -0.05 ± 0.07 for central fixation and -0.09 ± 0.06 for eccentric fixation, with the confidence intervals overlapping almost completely.

Blocked design

To further examine the spatiotopic properties of MT, we measured BOLD responses to stimuli over a range of four screen positions and for three different gaze directions (**Fig. 4**) using a blocked design and highly salient motion stimuli. Subjects maintained fixation on one of the three fixation points and stimuli appeared in one of four positions (chosen at random) for a duration of 15 s. The stimuli were random dots, moving coherently either upwards or downwards (direction randomized). Subjects were not instructed to attend to the stimulus and there was no task to encourage them to do so.

Figure 4 shows BOLD responses for the three gaze positions, plotted both as a function of retinal eccentricity (**Fig. 4a–d**) and as a function

Table 1 Talairach coordinates of the centroids of the retinotopic MT activation for the seven subjects of this study

	MT – L			MT – R		
	x	y	z	x	y	z
AT	-41	-70	0			
GDA	-42	-70	-1	48	-65	0
MCM	-48	-63	3	45	-65	2
CS	-40	-66	1	44	-66	-2
MC	-34	-66	8	42	-56	3
RC	-47	-60	6	48	-64	8
DRE	-36	-60	-3	39	-64	0

The average activation volume for left MT was 0.58 cm^3 and that for right MT was 0.62 cm^3 .

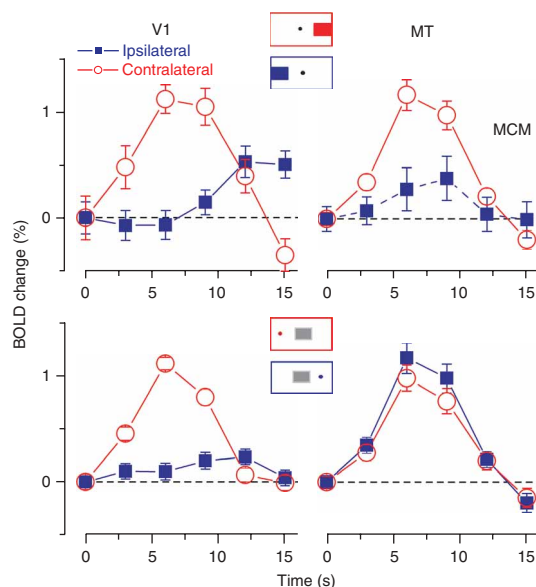


Figure 2 Time courses of the BOLD response to contralateral (red symbols) and ipsilateral stimuli (blue symbols) in the left V1 and the left retinotopic MT with central and lateral fixation. For V1 the ipsilateral response was always negligible for both central and lateral fixations. For MT, however, the response depended on gaze direction. The icons in the center illustrate the position of the stimulus and gaze (color coded for ipsi- and contralateral stimulation). Each data point shows the mean BOLD signal and the standard error, estimated from more than 50 independent stimulus presentations.

of external (screen) space (Fig. 4e–h). In V1, gaze did not alter the retinotopicity of the response: the response curves for the three different fixations are almost identical when plotted in retinal coordinates, but are widely separated when plotted in screen coordinates, both for subject CR and for the averaged data. MT, on the other hand, showed the opposite behavior. The curves were widely displaced in retinal coordinates, but almost lined up in spatial coordinates, showing a clear selectivity for the contralateral region of visual space.

For each hemisphere of each subject we calculated an index of spatiotopicity, defined as the amount of spatial shift (expressed as a proportion of gaze eccentricity) necessary to best align the eccentric-fixation response curves (Fig. 4) with the central-fixation curve (details in Methods). An index of zero implies no shift (in screen coordinates), which corresponds to spatiotopic tuning. An index of +1 means that the best shift was of the same direction and magnitude as the gaze shift, implying retinotopic selectivity. For V1 they scatter around unity (mean 0.99 ± 0.02 s.e.m.), indicating perfect retinotopicity (Fig. 5). For MT, however, the indexes were much closer to zero (mean 0.17 ± 0.04), with no value being greater than 0.3. There was a slight tendency for regions in the right hemisphere to be more spatiotopic than those in the left (spatiotopic index 0.09 ± 0.03 compared with 0.25 ± 0.03 ; $P = 0.02$, Student's t 2-tailed paired test). We also calculated the best shifts for the averaged data, yielding indexes of 1.00 for V1 and 0.10 for MT (Fig. 5). These data imply that for MT, but not V1, spatial tuning is invariant in a spatiotopic rather than in a retinotopic reference frame.

As mentioned earlier, gaze can affect neural response in various ways, including a shift of the receptive field in retinal coordinates² or multiplicative modulation of response gain^{3–5}. Inspection of the response curves (Fig. 4) suggests that their amplitudes do not change with fixation, but that the curves slide along the eccentricity axis. To distinguish quantitatively whether the gaze dependence of the MT tuning curves is best explained by either a shift of the receptive field or gain modulation of the neural response, we measured the degree to which these two models reduced the squared difference between the spatial profiles of the BOLD response in the eccentric-fixation and central-fixation conditions of the subject-averaged data (Fig. 4d). With both models, the curve transformations for left- and right-gaze conditions were coupled. For the shift model, the two eccentric conditions

were shifted together in opposite directions; for the gain model, one curve was multiplied while the other divided, by the same factor, which is consistent with the reported quasi-linear relationship between gaze and gain¹. The best spatial shift (index 0.1) reduced the squared difference by 90%, whereas the best multiplicative gain reduced squared difference by only 30%. Thus it would seem that for these data, the shift model is more appropriate. For V1 the best shift reduced the variance by only 2% and best gain by 18%, showing that no measurable eye-position effects are present in V1.

Different gaze directions are necessarily associated with different retinal projections of the display frame, which in turn may affect MT responses. If this were true, however, the response in V1 should also be affected, but it was not. For the single event experiment we calculated the coordinates of the centroids of the occipital responses along the calcarine fissure (excluding the first 3 mm of the midsagittal plane) to stimuli in all gaze conditions. The coordinates of the centroids did not change appreciably with gaze, shifting on average by 0.15, 0.4 and 1.5 in x , y and z Talairach coordinates, which was less than the images sampling size. This shows that the retinal positions of the border of the goggles had virtually no effect on the BOLD response in V1 and therefore probably did not affect the response in MT. In any event, it is hard to imagine how any such spurious responses could generate the specific spatial selectivity shown in Figure 4.

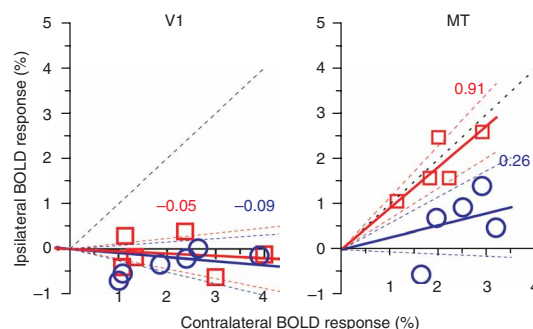


Figure 3 Amplitude of BOLD responses in V1 and MT to ipsilateral stimuli plotted against responses to contralateral stimuli. Each point shows the average BOLD response for each responsive hemisphere of three subjects. Blue points indicate central gaze with eccentric stimuli and red points indicate central stimuli with eccentric gaze. For V1 the ipsilateral response was always near zero. In MT, however, the ipsi- and contralateral responses were very similar when the stimuli were displayed centrally (spatiotopically), although there was a clear contralateral preference when fixation was maintained centrally and the stimuli were displaced. The solid red and blue lines are linear regressions, whose slopes characterize the average ratio of ipsilateral to contralateral response under various conditions. The dashed red and blue lines show the 95% confidence intervals for the linear fit. The regression slopes for V1 were -0.05 ± 0.06 and -0.09 ± 0.06 for central and lateral fixations, respectively, with the confidence bands overlapping almost completely. For MT the slopes were 0.91 ± 0.08 and 0.26 ± 0.11 , respectively, with no overlap between the 95% confidence intervals.

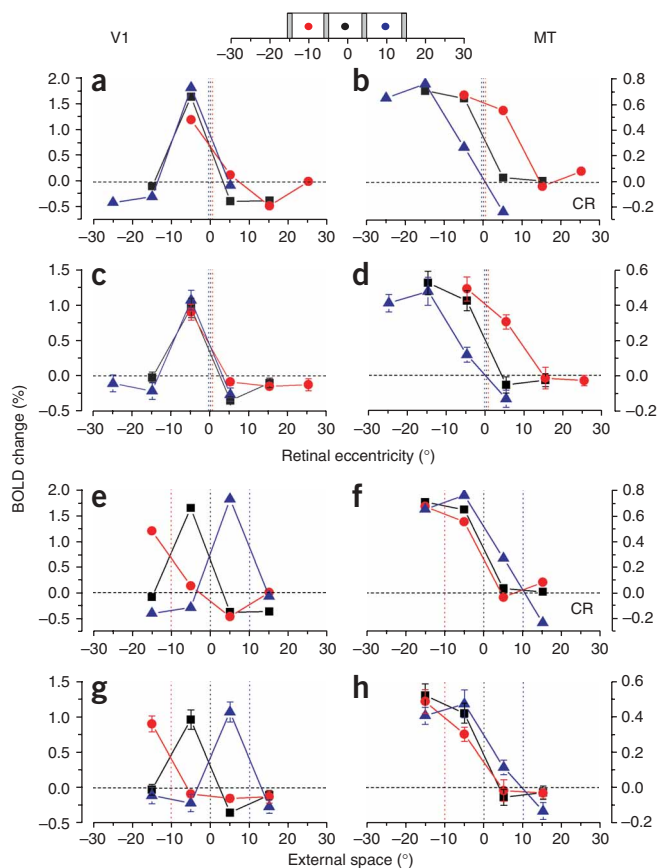


Figure 4 V1 (left) and MT (right) BOLD responses as a function of stimulus position for three different fixations. The upper inset illustrates the stimulus configuration: random dot patterns moved upwards or downwards in a $1^\circ \times 8^\circ$ window that was positioned in one of the four indicated positions ($\pm 5^\circ$ or $\pm 15^\circ$, with respect to the screen center). The three fixation points (0 and $\pm 10^\circ$) are indicated by the colored circles. (**a–d**) BOLD responses plotted in 'retinal' space, where 0 corresponds to the fovea and positive numbers to hemi-retina contralateral to the recorded hemisphere (projecting to ipsilateral space). (**e–h**) BOLD responses plotted in external space, where 0 corresponds to the screen center and positive distance refers to the distance on the screen ipsilateral to the hemisphere. **a, b, e, f** show the responses of the right hemisphere of observer CR and **c, d, g, h** show the average over hemispheres and subjects. The dotted vertical lines show the points of fixation (screen coordinates of 0 or $\pm 10^\circ$) and the curves of corresponding color show the BOLD responses at that fixation (red: -10° , black 0° , blue $+10^\circ$). The mean responses were calculated by averaging the visual responses from homologous regions of the two hemispheres for mirror symmetric fixation directions and stimulus positions. Error bars report the s.e.m. between subjects. These data show that, whereas the responses of V1 for different gaze positions line up well when plotted in retinal, but not in external space, those of MT line up better in external space.

DISCUSSION

Using two different stimulus configurations and two different experimental designs, this study shows that the magnitude of the activation in the so-called retinotopic portion of area MT depends not only on the retinal coordinates of the visual stimulus, but also on gaze direction. Identical retinal stimulation gave rise to a completely different pattern of selectivity when gaze was varied, causing the MT BOLD response to be invariant in a spatiotopic (or at least craniotopic) reference frame, but not in a retinotopic frame.

Spatiotopic selectivity was observed both for weakly coherent, near threshold motion signals and for highly salient motion signals. It was seen when observers were required to pay attention to the stimuli to judge direction and when stimuli were task irrelevant. We therefore conclude that attention is unlikely to be important in generating spatiotopic responses. Similarly, the spatiotopic effects cannot be attributed to eye movement artifacts, as the data for the different fixation conditions were collected in separate scans with the eyes still and the variance in fixation was not affected by gaze eccentricity (see Methods). Nor is it likely that the effort of maintaining eccentric fixation caused the results, as the effects of leftward fixation were quite different from rightward fixation (Fig. 4).

Single-unit physiological studies point to two possible mechanisms for achieving spatiotopic selectivity: a spatial shift of the receptive field or a multiplicative modulation of response gain (gain fields). Our results suggest that, at the population level, the effects of eye position on MT BOLD responses are better described by a shift in spatial tuning than by a change in response gain. It must be stressed, however, that the BOLD activity reflects population responses, not the responses of individual neurons. Individual neurons in human MT could well

show gain fields and indeed these may be the mechanism by which spatiotopic selectivity is created (as suggested previously²). As single-unit studies have shown that MT neurons in monkeys do have gain fields²⁸ similar to those reported in many other cortical areas, this idea is quite plausible. It has also been shown that single neurons in macaque MT (with relatively small receptive fields) can respond to remote visual stimulation in the ipsilateral field, if relevant to the task²⁹, which provides further evidence that MT receptive fields are highly dynamic and susceptible to reorganization by extraretinal and top-down signals. This study confirms that the human MT response is modulated by gaze, in a way that is consistent with spatiotopic selectivity.

In humans there is good, but indirect, psychophysical evidence for the existence of spatiotopic neurons from both adaptation^{14,30,31} and integration studies^{15,32}. These studies reveal spatiotopic encoding for some higher-level properties, such as face perception, but strictly

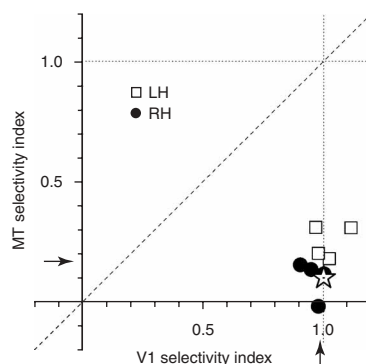


Figure 5 Index of spatiotopicity for areas MT and V1 for the left (open squares) and right (filled circles) hemispheres of four observers. The arrows near the axes show the mean value of the indexes, computed separately from the profiles of the individual hemispheres. The star symbol shows the index calculated from spatial profiles that were grand-averaged over all hemispheres (0.10 for MT, 1.00 for V1). An index of $+1$ implies that the area was perfectly retinotopic and an index of 0 implies that it was perfectly spatiotopic. The index was defined as the amount of spatial shift (expressed as a proportion of fixation eccentricity) necessary to best align the eccentric-fixation response curves (like the red and blue curves of Figs. 4c,d) with the central-fixation (black) curve (see Methods).

retinotopic encoding for adaptation to simpler attributes, such as contrast perception. The evidence for a spatiotopic adaptation pattern for high-level attributes is reinforced by a recent functional magnetic resonance imaging (fMRI) study showing the spatiotopic adaptation of BOLD signals in area LO, which is thought to mediate object recognition³³. Perhaps more surprising is the result that a simple task of direction discrimination, thought to be mediated by quite basic low-level mechanisms, shows spatiotopic (and also retinotopic) trans-saccadic integration¹⁵. The current fMRI results combine well with this psychophysical result, showing that human MT, which is important in motion analysis, has a spatial selectivity that seems to be anchored to an external, rather than a retinal, reference frame. This may be instrumental in constructing a spatially coherent, but dynamic, representation of the world in the face of continual eye movements.

METHODS

Subjects. Seven healthy adults took part in the study. All subjects were experienced in psychophysical procedures and had corrected-to-normal vision. Each subject gave informed consent prior to participation in accordance with the guidelines of the Human Studies Review Board of the Stella Maris Pediatric Neuropsychiatric Hospital. Each subject was scanned for 5 h or more, over several days.

Motion and retinotopic localizer. Fifty circular dots (1° diameter), half dark and half light, were displayed within a circular aperture of 20° diameter on a gray background. Each dot had a lifetime of 300 ms, encompassing 18 frames at a refresh rate of 60 Hz. Locally, the dots moved along linear trajectories at a constant speed of 7° s^{-1} . Three types of coherent motion were used: translation and rotation (inverting direction every 2 s) and gradually changing flow fields (for a detailed description see ref. 21). These coherent flow fields were followed by incoherent flow fields, with local velocities matched to those of the coherent stimulus. One full period of the display was 60 s. The different types of coherent flow (in different scans) were designed to maximize the extent of activation in area MT²². For each subject, the localization of MT was based on data obtained in at least seven scans.

A second localizer was used to identify activation that was modulated by a peripheral visual stimulus. Stimuli, comprising 50 randomly moving dots (9° diameter, limited lifetime of two frames), were presented for 6.0 s within a 4.5° square aperture, centered either 7.5° left or right of a central fixation marker (presentation order was randomized). This noise stimulus produced a strong response in human MT. After the 6 s of stimulus presentation, only the fixation point remained on the screen; the subsequent stimulus appeared with stimulus onset asynchrony (SOA) of 15, 18 or 21 s. These long times allowed us to estimate the time-course of the BOLD response on a trial by trial basis. Subjects maintained fixation throughout the session.

Widely spaced event-related design. In this study the stimulus was similar to the second localizer, except that the SOA was varied between 27 and 36 s, to allow both the separation of the stimulus-evoked BOLD response from the response associated with the key-press (at least 15 s after stimulus offset) and to allow the BOLD response to return to baseline before the following trial began. The stimulus and gaze positions were varied over four possible conditions, blocked in scans: central fixation with stimulus at $\pm 7.5^\circ$ eccentricity and central stimulus with fixation at $\pm 7.5^\circ$ eccentricity. The stimuli (confined within a $4.5^\circ \times 4.5^\circ$ square) comprised 6 s of dynamic random noise (two-frame lifetime), in which a brief (200- or 400-ms), near-threshold, vertical motion sequence was inserted. Motion coherence (proportion of signal to total dots within the motion signal) was adjusted individually to produce a correct response average of about 80% (on average 40% motion coherence). Fifteen seconds after stimulus offset a tone prompted subjects to indicate motion direction by pressing the appropriate hand-held response key. Three subjects participated in this experiment, with 45–75 functional scans per subject.

Blocked design. Four stimulus positions and three fixation positions were used for a total of 12 conditions (Fig. 4). Subjects maintaining fixation on one of three fixation spots, positioned either at the screen center (0°) or 10° left or

right of the screen center. Stimuli appeared randomly at one of four screen locations (-15° , -7.5° , 7.5° , 15°) in a rectangular aperture of $1^\circ \times 8^\circ$ for a duration of 15 s. Stimuli were comprised of 48 randomly positioned dots of maximum contrast (half white and half black), all moving coherently either upward or downward (direction chosen at random, two-frame limited lifetime, 15° s^{-1}). The SOA varied between 18, 21 and 24 s. After the stimulus had been presented at all four screen locations, the fixation mark was displaced to a new location and a new sequence of stimulus presentations began (after a 30-s blank interval to allow the BOLD signal to return to baseline). In each scan, all 12 conditions were presented once. Four subjects took part in this experiment, with 25 separate functional scans from each subject.

Stimulus presentation and eye-movement recording. Stimuli were presented on LCD goggles (Resonance Technology) with a visual field of $24^\circ \times 32^\circ$ at a luminance of about 30 candela per m^2 . The resolution of the display was 600×800 pixels with a refresh rate of 60 Hz. The goggles were equipped with an infrared camera to monitor eye position (sample frequency of 60 Hz, Arlington Research Software). The program checked that eye position did not drift by more than 1° (which never occurred in practice). We also performed an offline analysis of samples of the two-dimensional eye movement traces for three subjects to look for differences between the central and eccentric gaze conditions. There were no statistical differences between the variances of the eye traces in any of the subjects in any of the conditions (unpaired *t*-tests, $P > 0.1$ in all cases), suggesting that the stability of fixation did not depend on gaze direction. The average spread of eye position around fixation (across subjects and conditions) was $0.57 \pm 0.11^\circ$.

Imaging methods. A 1.5-T General Electronic Sigma Horizon System (General Electric) system provided full-brain anatomical three-dimensional high-resolution T1-weighted structural images (TR 21.1 ms, TE 3.8 ms, TI 700 ms, flip angle 10° ; receiver bandwidth 9.62 kHz; field of view $240 \times 240 \text{ mm}^2$; matrix 256×256 (1.1 mm thickness); 124 slices, 12 min acquisition time). BOLD functional data were collected using T2*-weighted echo-planar imaging gradient-recalled echo sequence (TR 3 s, TE 50 ms, flip angle 90° ; field of view $240 \times 240 \text{ mm}^2$; matrix 64×64 ; in-plane resolution 3.75 mm). For the first localizer (flow-motion) a total of 64 functional volumes were obtained in each scan. For the second localizer and the event-related study, 132 volumes were obtained in each scan. For the blocked design study, 112 volumes were acquired in each scan.

fMRI data analysis. We used two different software packages to analyze the BOLD response: noncommercial software (4DFP and FIDL) from Washington University for the widely spaced event-related design; Brain Voyager QX (version 1.7, Brain Innovation) for the blocked design. In both experiments functional data were temporally interpolated and re-sampled to compensate for systematic slice-dependent time differences. Odd-even slice intensity differences resulting from the interleaved acquisition were eliminated. The overall image intensity mode was normalized within scans to a standard value to compensate for interscan intensity differences. The data were realigned to the first volume of each scan, using a six-degree-of-freedom rigid-body affine transformation, to compensate for head motion during the scanning procedure. The functional data were transformed into a standard coordinate system³⁴. The three-dimensional reconstruction of individual anatomy was obtained from averages of at least four high-resolution structural images. At the end, the data were spatially re-sampled to a cubic voxel with a linear size of 3.0 mm (ref. 35).

BOLD time-series statistical analysis. *Widely spaced event-related design.* All data were analyzed using an assumed hemodynamic response, obtained by convolving the duration of the stimulus with an impulse response function³⁶. The amplitude of the response was estimated by fitting a general linear model to the BOLD time-series over all of the scans and sessions. For each scan the independent variables also included a constant, a linear term and a set of low-frequency cosine functions (cutoff frequency 0.009 Hz) to remove slow varying modulations of the BOLD signal³⁷. The percentage of BOLD signal modulation was calculated as the ratio of the BOLD signal amplitude to the constant term, averaged over scans. In the motion localizing scans, a *t*-test highlighted voxels in which the flow stimulus generated a greater BOLD response than the random motion display. In the retinotopic localizer, an unpaired *t*-test identified areas in which the visual stimulus in the left visual field elicited a



greater response than the stimulus in the right visual field. In the right hemisphere of subject AT it was not possible to locate a region with a strong preference for the contralateral visual field. This localizer was also used to map retinotopically responsive voxels along the calcarine sulcus, corresponding to the stereotypical anatomical localization of V1 (ref. 38), with little variation across subjects (although we cannot rule the possibility of slight contamination with portions of V2).

The BOLD response was estimated without a priori assumptions regarding the shape of its time course. Twelve consecutive delta functions were used to estimate the BOLD response to each stimulus. An estimate of the BOLD signal over the first ten frames of each trial was obtained by subtracting the estimated effects of the nuisance parameters and the estimate of the last one or two points of the previous trial average response, when they overlapped with the initial frames of the trial³⁷. The BOLD response time course was filtered by calculating the principal components over all trials and conditions and summing only the first five components. This procedure further removed high-frequency components of the BOLD signal that were not time-locked to stimulus onset³⁹. Summing all components did not alter the major pattern of the results. From the single trial data we calculated the standard error of the average BOLD amplitude within subjects. The data reported in **Figure 3** are the average signed deviation of the BOLD signal of the initial four frames from its value in the first frame. To recover the cortical surface for display purposes, the white matter–gray matter junction was traced and a fiducial surface midway through the cortical surface was generated using the SureFit method⁴⁰. An automatic algorithm, supplemented by manual correction by an expert operator, removed the errors generated by the initial segmentation. Each hemisphere's reconstruction was inflated and used for a surface-based representation of the statistical data.

Blocked design. Functional data were corrected for three-dimensional motion and the time courses in each voxel were corrected for linear drift and temporally smoothed (Gaussian kernel with a 2.8-s full width at half maximum). BOLD images were realigned and spatially normalized according to the atlas of Talairach and Tournoux³⁴ to obtain standardized coordinates for the regions of interest. Again we used a general linear model with a predictor convolved with the hemodynamic response for each of the 12 stimulus conditions (15 s), one blank condition (24 s) and one saccade condition (6 s). We coded separately the responses to the blank condition for each fixation, found no difference between them and therefore pooled them. To generate functional maps, we computed the intersection of two general linear model contrasts. The first contrast identified voxels that were more active in response to the contralateral stimulus with respect to the ipsilateral for the central fixation ($P \leq 0.01$). The second contrast compared the activation of the coherent flow motion versus random motion ($P \leq 0.05$). We only labeled clusters of three or more contiguous voxels. Maps were superimposed on three-dimensional anatomical reference scans. We calculated the modulation of the averaged BOLD response to each stimulus, gaze position and hemisphere by subtracting from the mean modulation of the first 12 s after the stimulus presentation that of the 6 s preceding the stimulus presentation. This technique reduces subject variability.

We also calculated mean BOLD responses across subjects by averaging contralateral responses with contralateral responses, and contralateral gaze conditions with contralateral gaze conditions, etc. For example, the right-fixation (ipsi-fixation) condition of the right hemisphere was averaged with the left (ipsi)-fixation condition of the left hemisphere and the response to stimuli at $+15^\circ$ of the left hemisphere (contralateral stimulation) was averaged with that of the response to stimuli at -15° (contralateral) of the right hemisphere. The errors reported in **Figure 4** are the s.e.m. across subjects.

To evaluate the spatiotopic behavior of an area, we defined an index based on the amount of retinotopic shift required to best align the BOLD response curves of the three different fixations (**Fig. 4**). The curves of BOLD amplitude versus stimulus position were linearly interpolated to a precision of 100 points per degree, extrapolating 5° on either side. The interpolated curves for the eccentric-fixation conditions were then rigidly displaced in tandem along the space axis, in opposite directions (shifts towards fixation defined as positive). For each displacement, the BOLD amplitudes for the eccentric-fixation curves were subtracted from those of the central curve to calculate the sum of squared residuals. The dimensionless spatiotopic index was taken as the displacement

(in degrees) that minimized the total sum squared residuals, divided by the magnitude of eccentric gaze direction (in degrees).

ACKNOWLEDGMENTS

We thank A. Snyder and M. McAvoy of the Washington University Neuro-Imaging laboratory for making available the preprocessing and statistical analysis software and for continual technical assistance. The project was supported by the Italian Ministry for Research (Ministero Italiano della Università e Ricerca, Progetti di Ricerca di Interesse Nazionale 2005), the European Commission Sixth Framework Program (New and Emerging Science and Technology grant 'MEMORY') and the Australian National Health and Medical Research Council (NHMRC project grant 303133).

COMPETING INTERESTS STATEMENT

The authors declare that they have no competing financial interests.

Published online at <http://www.nature.com/natureneuroscience>

Reprints and permissions information is available online at <http://npg.nature.com/reprintsandpermissions>

- Andersen, R.A., Essick, G.K. & Siegel, R.M. Encoding of spatial location by posterior parietal neurons. *Science* **230**, 456–458 (1985).
- Zipser, D. & Andersen, R.A. A back-propagation programmed network that simulates response properties of a subset of posterior parietal neurons. *Nature* **331**, 679–684 (1988).
- Galletti, C., Battaglini, P.P. & Fattori, P. Parietal neurons encoding spatial locations in craniotopic coordinates. *Exp. Brain Res.* **96**, 221–229 (1993).
- Galletti, C., Battaglini, P.P. & Fattori, P. Eye position influence on the parieto-occipital area PO (V6) of the macaque monkey. *Eur. J. Neurosci.* **7**, 2486–2501 (1995).
- Duhamel, J., Bremmer, F., BenHamed, S. & Graf, W. Spatial invariance of visual receptive fields in parietal cortex neurons. *Nature* **389**, 845–848 (1997).
- Sereno, M.I. & Huang, R.S. A human parietal face area contains aligned head-centered visual and tactile maps. *Nat. Neurosci.* **9**, 1337–1343 (2006).
- Bremmer, F. *et al.* Polymodal motion processing in posterior parietal and premotor cortex: a human fMRI study strongly implies equivalencies between humans and monkeys. *Neuron* **29**, 287–296 (2001).
- Buneo, C.A., Jarvis, M.R., Batista, A.P. & Andersen, R.A. Direct visuomotor transformations for reaching. *Nature* **416**, 632–636 (2002).
- Pouget, A., Deneve, S. & Duhamel, J.R. A computational perspective on the neural basis of multisensory spatial representations. *Nat. Rev. Neurosci.* **3**, 741–747 (2002).
- Avillac, M., Deneve, S., Olivier, E., Pouget, A. & Duhamel, J.R. Reference frames for representing visual and tactile locations in parietal cortex. *Nat. Neurosci.* **8**, 941–949 (2005).
- Nakamura, K. & Colby, C.L. Updating of the visual representation in monkey striate and extrastriate cortex during saccades. *Proc. Natl. Acad. Sci. USA* **99**, 4026–4031 (2002).
- Duhamel, J.R., Colby, C.L. & Goldberg, M.E. The updating of the representation of visual space in parietal cortex by intended eye movements. *Science* **255**, 90–92 (1992).
- Merriam, E.P., Genovesi, C.R. & Colby, C.L. Spatial updating in human parietal cortex. *Neuron* **39**, 361–373 (2003).
- Melcher, D. Spatiotopic transfer of visual-form adaptation across saccadic eye movements. *Curr. Biol.* **15**, 1745–1748 (2005).
- Melcher, D. & Morrone, M.C. Spatiotopic temporal integration of visual motion across saccadic eye movements. *Nat. Neurosci.* **6**, 877–881 (2003).
- Zohary, E., Shadlen, M.N. & Newsome, W.T. Correlated neuronal discharge rate and its implications for psychophysical performance. *Nature* **370**, 140–143 (1994).
- Britten, K.H., Shadlen, M.N., Newsome, W.T. & Movshon, J.A. The analysis of visual motion: a comparison of neuronal and psychophysical performance. *J. Neurosci.* **12**, 4745–4765 (1992).
- Zeki, S. *et al.* A direct demonstration of functional specialization in human visual cortex. *J. Neurosci.* **11**, 641–649 (1991).
- Tootell, R.B. *et al.* Visual motion aftereffect in human cortical area MT revealed by functional magnetic resonance imaging. *Nature* **375**, 139–141 (1995).
- Rees, G., Friston, K. & Koch, C. A direct quantitative relationship between the functional properties of human and macaque V5. *Nat. Neurosci.* **3**, 716–723 (2000).
- Morrone, M.C. *et al.* A cortical area that responds specifically to optic flow, revealed by fMRI. *Nat. Neurosci.* **3**, 1322–1328 (2000).
- Huk, A.C., Dougherty, R.F. & Heeger, D.J. Retinotopy and functional subdivision of human areas MT and MST. *J. Neurosci.* **22**, 7195–7205 (2002).
- Smith, A.T., Wall, M.B., Williams, A.L. & Singh, K.D. Sensitivity to optic flow in human cortical areas MT and MST. *Eur. J. Neurosci.* **23**, 561–569 (2006).
- DeSouza, J.F., Dukelow, S.P. & Vilis, T. Eye position signals modulate early dorsal and ventral visual areas. *Cereb. Cortex* **12**, 991–997 (2002).
- Goossens, J., Dukelow, S.P., Menon, R.S., Vilis, T. & van den Berg, A.V. Representation of head-centric flow in the human motion complex. *J. Neurosci.* **26**, 5616–5627 (2006).
- Bradley, D.C., Maxwell, M., Andersen, R.A., Banks, M.S. & Shenoy, K.V. Mechanisms of heading perception in primate visual cortex. *Science* **273**, 1544–1547 (1996).
- Denys, K. *et al.* The processing of visual shape in the cerebral cortex of human and nonhuman primates: a functional magnetic resonance imaging study. *J. Neurosci.* **24**, 2551–2565 (2004).

28. Bremmer, F., Ilg, U.J., Thiele, A., Distler, C. & Hoffmann, K.P. Eye position effects in monkey cortex. I. Visual and pursuit-related activity in extrastriate areas MT and MST. *J. Neurophysiol.* **77**, 944–961 (1997).
29. Zaksas, D. & Pasternak, T. Area MT neurons respond to visual motion distant from their receptive fields. *J. Neurophysiol.* **94**, 4156–4167 (2005).
30. Nishida, S., Motoyoshi, I., Andersen, R.A. & Shimojo, S. Gaze modulation of visual aftereffects. *Vision Res.* **43**, 639–649 (2003).
31. Nieman, D.R., Hayashi, R., Andersen, R.A. & Shimojo, S. Gaze direction modulates visual aftereffects in depth and color. *Vision Res.* **45**, 2885–2894 (2005).
32. Hayhoe, M., Lachter, J. & Feldman, J. Integration of form across saccadic eye movements. *Perception* **20**, 393–402 (1991).
33. McKyton, A. & Zohary, E. Beyond retinotopic mapping: the spatial representation of objects in the human lateral occipital complex. *Cereb Cortex*, published online 3 July 2006 (doi:10.1093/cercor/bh1027).
34. Talairach, J. & Tournoux, P. *Stereotactic Coplanar Atlas of the Human Brain* (Thieme Medical Publishers, New York, 1988).
35. Fox, M.D., Snyder, A.Z., Barch, D.M., Gusnard, D.A. & Raichle, M.E. Transient BOLD responses at block transitions. *Neuroimage* **28**, 956–966 (2005).
36. Boynton, G.M., Engel, S.A., Glover, G.H. & Heeger, D.J. Linear systems analysis of functional magnetic resonance imaging in human V1. *J. Neurosci.* **16**, 4207–4221 (1996).
37. Ollinger, J.M., Corbetta, M. & Shulman, G.L. Separating processes within a trial in event-related functional MRI. *Neuroimage* **13**, 218–229 (2001).
38. Hasnain, M.K., Fox, P.T. & Woldorff, M.G. Intersubject variability of functional areas in the human visual cortex. *Hum. Brain Mapp.* **6**, 301–315 (1998).
39. d'Avossa, G., Shulman, G.L. & Corbetta, M. Identification of cerebral networks by classification of the shape of BOLD responses. *J. Neurophysiol.* **90**, 360–371 (2003).
40. Van Essen, D.C. *et al.* An integrated software suite for surface-based analyses of cerebral cortex. *J. Am. Med. Inform. Assoc.* **8**, 443–459 (2001).